Ingeniería Investigación y Tecnología
volumen XXIV (número 2), abril-junio 2023 1-9
ISSN 2594-0732 FI-UNAM artículo arbitrado
Información del artículo: Recibido: 8 de septiembre de 2020, reevaluado: 25 de enero y 8 de septiembre de 2022, aceptado: 7 de febrero de 2023

https://doi.org/10.22201/fi.25940732e.2023.24.2.016

Ingeniería Investigación y Tecnología

Cancellation of inertial effects in 1 degree of freedom mechanisms applying sliding mode control with response in finite time

Cancelación de efectos inerciales en mecanismos de 1 grado de libertad aplicando control por modos deslizantes con respuesta en tiempo finito

Suárez-Calderón Juan Carlos
Instituto Politécnico Nacional
E-mail: jcarlos.suarez@live.com
https://orcid.org/0000-0003-3152-3018

Susarrey-Huerta Orlando
Instituto Politécnico Nacional
E-mail: osusarrey@yahoo.com
https://orcid.org/0000-0003-3347-6438

Desiderio-Maya Daniela
Instituto Politécnico Nacional
E-mail: danieladmaya@outlook.com
https://orcid.org/0000-0002-8787-8953

Rocha-Gómez Iván
Instituto Politécnico Nacional
E-mail: ivanrocha.go@gmail.com
https://orcid.org/0000-000293682762

Flores-Campos Juan Alejandro
Instituto Politécnico Nacional
E-mail: alejandro.jhane@gmail.com
https://orcid.org/0000-0002-1632-7716

Abstract

Canceling the effects generated by inertia in the mechanisms is a complicated task with great benefits, such as reducing the chattering effect and, in turn, energy consumption. This paper proposed a control method for electromechanical systems with one degree of freedom. The proposed method guarantees robustness, reaching a desired position in a finite time through the application of a control law using sliding modes with Time Base Generator (TBG) and the cancellation of the effects produced by inertia. The speed belongs to Gaussian bell-shape profile, then the speed has a normal distribution from energy used during the displacement, which allows the control algorithm to be applied in tasks such as feeding parts in processes that require precision or in painting processes, since the behavior of the speed is similar to the speed of the human limbs. The contribution is a robust control algorithm that can be adapted to any one degree of freedom mechanism that has the task of reaching a position in a specific time, the time begin determined by the user. The algorithm eradicates speed fluctuations, so over-acceleration is zero and disturbances generated by loads applied to the mechanism are also compensated.
Keywords: Chattering free, inertial effects, sliding modes, time base generator, one degree of freedom mechanism.

Resumen

Cancelar los efectos producidos por la inercia en los mecanismos es una tarea complicada que trae grandes beneficios, como son: La reducción del efecto denominado *chattering* y, al mismo tiempo, reducción en el consumo de energía. Este artículo propone una metodología de control para sistemas electromecánicos de un grado de libertad. La metodología propuesta garantiza robustez, busca alcanzar una posición deseada en un tiempo específico aplicando una ley de control que utiliza modos deslizantes y un generador de base de tiempo (TBG) cancelando con ello los efectos generados por la inercia. La velocidad presenta una forma de campana Gaussiana, es decir, la velocidad posee una distribución normal de energía durante el movimiento, lo que permite aplicar el algoritmo de control a tareas como: Alimentación de piezas en procesos que requieren precisión o procesos de pintura, ya que el comportamiento de la velocidad es similar a la velocidad descrita por las extremidades del cuerpo humano. La contribución es un algoritmo de control robusto que puede ser adaptado a cualquier mecanismo de un grado de libertad cuya tarea sea alcanzar una posición en un tiempo especificado por el usuario. Las fluctuaciones de velocidad son erradicadas por el algoritmo; en consecuencia, la sobre aceleración es nula y las perturbaciones generadas por las cargas aplicadas al mecanismo también son compensadas.
Descriptores: Efectos inerciales, efecto slinky, efecto Chattering, generador de tiempo base (TBG), sistemas de control, modos deslizantes, mecanismos de 1 GDL.

https://doi.org/10.22201/fi.25940732e.2023.24.2.016

Introduction

In recent years, many studies have focused on solving the problem of chatter-free mechanisms. On the other hand, new proposals have been made to obtain control algorithms capable of developing bell-shaped speed profiles whose task is to emulate the speed profiles described by human limbs. Tasks such as the transport of dangerous substances or liquids that can spill show the importance of eradicating inertial effects, achieving a bell-shaped speed profile.

For example, the way a human being generally moves his hand along a more or less straight path from one point to another shows common invariant kinematic features such as a bell-shaped speed profile (Morasso, 1981), many models have also been proposed; for example, "a minimal torque-change model" (Uno *et al.*, 1989), "a minimum jerk model" (Flash & Hogan, 1985), both models can generate hand trajectories in good agreement with the experimental data. Furthermore, in Yeung & Chen (1988) a variable structure model following control design (VSMFC) for robotic applications was presented in which the chattering problem was solved. In Chen *et al.* (1990) a control algorithm was proposed where the inverse of the inertial matrix was not required. Another method that uses an electrostatic potential field and a sliding mode for a manipulator that regulates the movement time but not the dynamic behavior of a robot has been presented in Hashimoto (1993). In addition, Morasso (1993) proposed a Time Base Generator (TBG) that generates a time series with a bell-shaped velocity profile, and showed that the trajectory of a hand can be generated with a transnational speed and rotational speed with a TBG signal.

On the other hand, Sira (1992) and Zhang & Panda (1999) have proposed an involved dynamic sliding mode control technique for a general class of nonlinear systems. However, the strict requirement of the measurement of the slip surface derivative is necessary, so Tsuji *et al.* (1995) proposed a method with a TBG in artificial potential field approach (APFA) that can regulate the time of motion and also the speed profile of the robot but it cannot be applied to dynamic control. In 1998, a new method is developed introducing the combination of a time scale transformation with a TBG, the method is useful for robot time scheduling problems (Tanaka *et al.*, 1998). In addition, a new stability analysis and design procedure for variable structure robotic controllers with PID-type sliding surfaces was presented, the controller is simple and robust (Stepanenco *et al.*, 1998).

A human-like trajectory is generated for the robots with the TBG-based trajectory generation method (Tanaka *et al.*, 1999), then the TBG generates a target spatial and temporal trajectory for the robot (Tanaka *et al.*, 2000). A novel chattering-free dynamic slip mode controller is proposed for a time-varying sliding regime for all times and for any initial conditions (Parra, 2001). Subsequently, a Cartesian control system is proposed in (Dominguez *et al.*, 2008), which guarantees a robust tracking in finite time based on a time base generator for uncertain robotic arms, to achieve this goal we proposed a nonlinear control based on modes second-order sliders, however this method only works on robots without gravity. Another alternative to reduce the inertial effects has been presented in (Kuo *et al.*, 2011). The chatter effect is addressed in García *et al.* (2011). On the other hand, a non-chattering sliding mode controller is proposed, the new sliding surface is parameterized by a base time generator (Gashemi & Nersesov, 2013). Chatter is a phenomenon that has been sought to eliminate through many methodologies, thus a new sliding mode controller with a continuous control strategy has been proposed to achieve a chattering-free controller (Feng *et al.*, 2014). A new controller with faster response and gravity compensation was introduced in Huang *et al.* (2014), Nonlinear Proportional Derivative (NPD) controller has smaller errors than conventional Proportional Derivative (PD) controllers.

In this paper we present a robust control algorithm for one degree of freedom mechanisms that solves the problem of inertial effects, eliminates chattering and presents a bell-shaped speed profile. The algorithm is based on a sliding mode control and a time base generator, the algorithm reaches a desired position in a finite time, the algorithm is adaptable to any mechanism of one degree of freedom and is applicable to tasks that require precision, the future scope of this research is to apply the algorithm to robotic arms, such as prostheses or mechanisms focused on rehabilitation, future studies to mechanisms of two or more degrees of freedom.

Modelling

Kinematic Model–vector Loop Method

This section presents the kinematic and dynamic analysis of a one degree of freedom mechanism. The mechanism has a rotary actuator that generates the displacement q in the point, and point is vertically displaced.

Figure 1 shows the kinematic constraint equation. R_1, R_2, and R_3 are the vectors that describe the loop equation (1).

$$R_1 = R_2 + R_3 \tag{1}$$

https://doi.org/10.22201/fi.25940732e.2023.24.2.016

The angles are defined with respect to the positive *X*-axis and the vectors are defined by equations (2), (3) and (4).

$$R_1 = (0,\ Y_h) \tag{2}$$

$$R_2 = AB\ (cos\ q,\ sin\ q) \tag{3}$$

$$R_3 = BC\ (cos\ \theta_3,\ sin\ \theta_3) \tag{4}$$

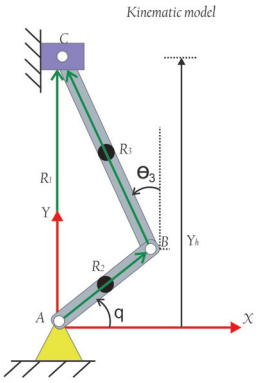

Figure1. Definition of the kinematic constraint equation

For position analysis we define the vector *P* as the unknown variables that determine the position.

$$[P] = \begin{bmatrix} \theta_3 \\ Y_h \end{bmatrix} \tag{5}$$

With the components of each position vector, the kinematic constraint functions (6) and (7) are obtained, the functions are equal to zero because the geometry of the mechanism is closed.

$$f_1 = R_2\ cos\ q + R_3\ cos\ \theta_3 = 0 \tag{6}$$

$$f_2 = R_2\ sin\ q + R_3\ sin\ \theta_3 - Y_h = 0 \tag{7}$$

With the kinematic constraints, the position matrix (8) is found, now it is possible to know the position of the mechanism at any time:

$$\begin{bmatrix} \theta_3 \\ Y_h \end{bmatrix} = \begin{bmatrix} \sin^{-1}\left(\dfrac{-R_2 \sin q + Y_h}{R_3}\right) \\ R_2 \cos q + R_3 \cos \theta_3 \end{bmatrix} \tag{8}$$

The kinetic energy of the mechanism is obtained from the velocity analysis, therefore *F* is the matrix of the kinematic constraint functions of the mechanism:

$$F = \begin{bmatrix} f_1 \\ f_2 \end{bmatrix} = \begin{bmatrix} R_2 \cos q + R_3 \cos \theta_3 \\ R_2 \sin q + R_3 \sin \theta_3 - Y_h \end{bmatrix} = \begin{bmatrix} 0 \\ 0 \end{bmatrix} \tag{9}$$

Differentiating the matrix of the kinematic constraint functions with respect to time, the velocity is obtained:

$$F = \begin{bmatrix} \dot{f}_1 \\ \dot{f}_2 \end{bmatrix} = \begin{bmatrix} -R_2 \sin q\, \dot{q} - R_3 \sin \theta_3\, \dot{\theta}_3 \\ R_2 \cos q\, \dot{q} + R_3 \cos \theta_3 \dot{\theta}_3 - \dot{Y}_h \end{bmatrix} = \begin{bmatrix} 0 \\ 0 \end{bmatrix} \tag{10}$$

From (10) the acceleration is derived:

$$F = \begin{bmatrix} \ddot{f}_1 \\ \ddot{f}_2 \end{bmatrix} = \begin{bmatrix} (-R_2 \sin q\ddot{q} + q \cos q\dot{q}) - (R_3 \sin \dot{\theta}_3\ddot{\theta}_3 + \dot{\theta}_3 \cos \theta_3\dot{\theta}_3) \\ (R_2 \cos q\ddot{q} - \dot{q} \sin q\dot{q}) + (R_3 \cos \theta_3\ddot{\theta}_3 - \dot{\theta}_3 \sin \theta_3\dot{\theta}_3) - \ddot{Y}_h \end{bmatrix} = \begin{bmatrix} 0 \\ 0 \end{bmatrix} \tag{11}$$

The matrices are solved using Wolfram Mathematica®.

Mechanism dynamics

The dynamic model of the mechanism used in this paper can be written as follows:

$$M(q')\ddot{q} + C(q', \dot{q}')\dot{q} + G(q') = U \tag{12}$$

Where $M(q')$ denotes a *nxn* symmetric positive definite inertial matrix, $C(q', \dot{q}')$ represents a *nxn* matrix of Coriolis and centrifugal forces, $G(q')$ models the gravity forces, and *U* is the torque input. The methodology by extended dynamics method, we have:

$$\dot{q}' = \rho(q')\dot{q} \tag{13}$$

$$q' = \sigma(q) \tag{14}$$

Therefore, substituting (13) and (14) in (12), the dynamic model components are rewritten as:

$$M(q') = \rho(q')^T M'(q')\rho(q')$$

$$C(q, \dot{q}') = \rho(q')^T C'(q', \dot{q}')\rho(q') + \rho(q')^T M'(q')\dot{\rho}(q', \dot{q}') \tag{15}$$

$$G(q') = \rho(q')^T G'(q') \tag{16}$$

Jacobian Extended:

$$\rho(q') = \begin{bmatrix} 1 \\ \dfrac{-R_2 csc(\theta_3) \sin(q)}{R_3} \\ R_2 \cos(q) + \cot(\theta_3) \sin(q) \end{bmatrix} \tag{17}$$

https://doi.org/10.22201/fi.25940732e.2023.24.2.016

Inertia Matrix:

$$M'(q') = \begin{bmatrix} J_2 + \frac{m_2 R_2^2}{4} + m_3 R_2^2 & \frac{1}{2} m_3 R_2 R_3 \cos(q-\theta_3) & 0 \\ \frac{1}{2} m_3 R_2 R_3 \cos(q-\theta_3) & J_3 + \frac{m_3 R_3^2}{4} & 0 \\ 0 & 0 & m_4 \end{bmatrix} \quad (18)$$

Matrix of centripetal and Coriolis forces:

$$C'(q',\dot{q}') = \begin{bmatrix} 0 & \frac{1}{2} m_3 R_2 R_3 \dot{\theta}_3 \sin(q-\theta_3) & 0 \\ \frac{-1}{2} m_3 \dot{q} R_2 R_3 \sin(q-\theta_3) & 0 & 0 \\ 0 & 0 & 0 \end{bmatrix} \quad (19)$$

Gravitational vector:

$$G'(q) = g \quad (20)$$

The dynamic model is solved with Wolfram Mathematica® and the solution is validated using: Working Model® *vs* Matlab-Simulink®. Figure 2 shows the validation of the dynamic model in terms of the generalized variable q. The simulation conditions are shown in Table 1.

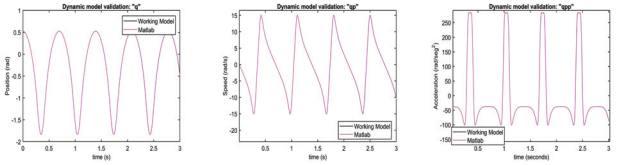

a) b) c)

Figure 2. Dynamic model validation: a) "q" position (q), b) "q" speed profile ($\dot{q}$) and c)" q" acceleration ($\ddot{q}$)

Table 1. Validation parameters of the dynamic model in the Matlab-Simulink software

Simulation parameters	Value
Tau (U)	0.001 Nm
Solver	O de 4 (Runge-Kutta)
Sampling time of simulation	3 s
Integration step	0.001

Figure 3a shows the position of the generalized variable q, the velocity of the generalized variable is shown in 3b and finally 3c shows the acceleration. The graphs in magenta color correspond to Matlab-Simulink®, while the graphs in black color correspond to the Working Model®. For all three cases the graphs converge.

Control algorithm

The algorithm presented in this paper is a robust technique for nonlinear systems that operate under conditions of uncertainty. The sliding mode control reduces the sensitivity to the variation of uncertainties and external disturbances.

Time base generator

The time base generator equation (22) is written as a time function (21), where $e(t)$ shows the error position, $\dot{e}(t)$represents the speed error, and $\alpha(t)$ is the time-varying feedback gain.
In addition, equation (21); being a non-forced time-varying function allows the time base generator to be analyzed like error function, being possible to combine it with the sliding mode control law.

$$\dot{e} + \alpha\,(t)\, e = 0 \rightarrow \dot{e} = -\,\alpha\,(t)\, e \quad (21)$$

Where:

$$\alpha(t) = \alpha_0 \frac{\dot{\xi}}{(1-\xi)+\delta} \quad (22)$$

In equation (22), ξ is a scalar variable as a function of time $\xi(t)$ whit a bell-shaped speed profile generated by the TBG as a time varying feedback gain. $\xi(t)$ is defined as a first differentiable non-increasing function satisfying $\xi(0) = 1$ and $\xi(t_f) = 0$, where t_f is the convergence time from the initial to target position. The dynamics of TBG will be used for determining the function of convergence time and is defined as follows (Tsuji, 1995):

$$\dot{\xi} = \gamma(\xi(1.0-\xi))^{\beta} \quad (23)$$

Where γ is defined as a function of the convergence time t_f and β is a constant that determines the behavior of TBG and $0 < \beta < 1$. From equation (23), $\xi(t)$ has two equilibrium points. Therefore, $\xi(t)$ always converges stably to $\xi(0)$, when an initial value of ξ is chosen as $\xi\,(0) = 1 - \varepsilon$ using a small positive constant ε.

$$t_f = \int_0^{tf} dt = \int_1^0 \frac{d\xi}{\dot{\xi}} = \frac{\Gamma^2(1-\beta)}{\gamma\,\Gamma(2-2\beta)} \quad (24)$$

In Tanaka *et al.* (1998) a new trajectory generation method for an omnidirectional mobile robot has been proposed, equation (24) has been used to generate a

composite time scale, where the convergence times are defined according with β. Therefore, equation (24) represents the convergence time, where $\Gamma(\cdot)$ is the Euler's integral of the second kind (gamma function). When the parameter γ is:

$$\gamma = \frac{\Gamma^2(1-\beta)}{t_f \Gamma(2-2\beta)} \tag{25}$$

The system converges to the equilibrium point in t_f. The speed profile $\dot{\xi}(t)$ satisfies $\dot{\xi}(0)$ and $\dot{\xi}(t_f) = 0$, and is bell-shaped with the minimum value $\dot{\xi}(t_f/2) = -\gamma 4^{-\beta}$ at $t = t_f/2$.

From (22), $\alpha_0 = 1 + \varepsilon$, $0 < \varepsilon, << 1$ *y* $0 < \delta << 1$

The time base generator must be defined by the designer of the controller, such that ξ moves from 0 to 1 in finite time. The gain $\alpha(t)$ is defined as $\alpha(t_f) > 0$, if t_f is independent of the initial conditions. Therefore:

$$\xi(t_f) = 1 \rightarrow e(t_f) = e(t_0)\,\delta^{1+\varepsilon} > 0 \tag{26}$$

The trajectory $\xi = \xi(t) \in C^2$ so as to ξ goes smoothly from 0 to 1, $t = t_f > 0$, and $\xi = \xi(t)$ is a bell-shaped derivative of ξ such that $\dot{\xi}(t_0) = \dot{\xi}(t_f) \equiv 0$, we have: $t = 0.5t_f$ is the maximum value and for the second derivative we have: $\ddot{\xi}(0.5t_f) \equiv 0$. Note that t_f independent of any initial condition and hence can be made arbitrarily small in arbitrary finite time. Also note that the transient state is shaped by $\xi(t)$ over time.

Therefore, equation (27), (28) and (29) show that the desired trajectory is fulfilled.

$$\xi(t) = \alpha_1 \frac{(t-t_0)^3}{(t_f-t_0)^3} - \alpha_2 \frac{(t-t_0)^4}{(t_f-t_0)^4} + \alpha_3 \frac{(t-t_0)^5}{(t_f-t_0)^5} \tag{27}$$

$$\dot{\xi}(t) = 3\alpha_1 \frac{(t-t_0)^2}{(t_f-t_0)^3} - 4\alpha_2 \frac{(t-t_0)^3}{(t_f-t_0)^4} + 5\alpha_3 \frac{(t-t_0)^4}{(t_f-t_0)^5} \tag{28}$$

$$\ddot{\xi}(t) = 6\alpha_1 \frac{(t-t_0)}{(t_f-t_0)^3} - 12\alpha_2 \frac{(t-t_0)^2}{(t_f-t_0)^4} + 20\alpha_3 \frac{(t-t_0)^3}{(t_f-t_0)^5} \tag{29}$$

Where the parameters assigned to demonstrate the trajectory are:

$$\xi(t_0) = 0, \xi(t_f) = 1, \dot{\xi}(t_0) = \dot{\xi}(t_f) = 0 \text{ y } \ddot{\xi}(0.5t_f) = 0$$

Now equations (27), (28) and (29) becomes the system (30).

$$\alpha_1 - \alpha_2 + \alpha_3 = 1$$

$$3\alpha_1 - 4\alpha_2 + 5\alpha_3 = 0$$

$$6\alpha_1 - 12\alpha_2 + 20\alpha_3 = 0$$

Then the system is solved, obtaining as a result: $\alpha_1 = 10$, $\alpha_2 = 15$, and $\alpha_3 = 6$ The time base generator is obtained with Matlab-Simulink®.

The results are shown in Figure 3, the convergence time is 5 seconds.

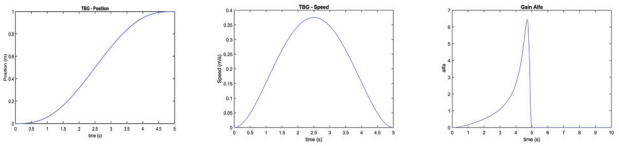

Figure 3. a) $\xi(t)$ position, b) $\dot{\xi}(t)$ speed trajectory and c) α gain

Figure 3 shows that the trajectories established in (21) and (22) are true, and this allows the mechanism to be taken from one point to another in a finite time. On the other hand, the α gain is responsible for bringing the error to zero in transient space in a finite time.

Sliding mode control

The position control is proposed in the joint space; where q is the position and qd is the target position (Figure 1). Therefore, the errors are:

$$e = q - qd \tag{31}$$

$$\dot{e} = \dot{q} - \dot{q}d \tag{32}$$

In this paper we introduce the TBG as a function of time (21) to the slip surface (33) with the intention of trapping the system in the stable state and not allowing disturbances, making the error smaller each time. Therefore, the sliding surface proposed for the control law is.

$$S = \dot{e} + \alpha(t)e \tag{33}$$

Substituting errors of position (31) and speed (32) in sliding surface (33), the new sliding surface can be written as:

$$S = (\dot{q} - \dot{q}d) + \alpha(t)(q - qd) \tag{34}$$

In Parra (2003) the sgn function is used to catch the error in the sliding surface, then the next equations have been proposed:

$$S_q = S - Sd \tag{35}$$

https://doi.org/10.22201/fi.25940732e.2023.24.2.016

Where S_q is the sliding surface in terms of Sd, where Sd represents the desired reference value. To bring the error to zero smoothy in transient we introduce Sd.

$$Sd = S(t_0)exp^{-k\,(t\,-\,t_0)} \tag{36}$$

In the equation (36), t represents the final time, t_0 the initial time, k is a positive constant, S is the sliding surface and $S(t_0)$ is the initial position and speed error when time $t = t_0 = 0s$.

Therefore, the sliding mode control law can be written as:

$$\tau = -\,sgn\,(S_q) \tag{37}$$

The control law that is applied is by sliding modes. The sgn function allows catch the error on the sliding surface, however, the tanh function a smoother displacement is obtained, which helps to reduce chattering in the motor.

$$\tau = tanh\,(S_q) \tag{38}$$

Therefore, the equation (38) is the control law, however to achieve more robust control a PID is applied. The PID is defined in a general way in (39).

$$U(v) = k_p e(v) + k_i \int e(v)dv + kd\,\frac{de(v)}{dv} \tag{39}$$

Where k_p, k_i and k_d are proportional gain, integral gain and derivative gain respectively. Therefore, the new law includes a PID + sliding surface with TBG is written as:

$$\tau = -\,k_p e - k_d\,\dot{e} + k_d Sd - k_i \int_{t_0}^{t} tanh\left(S_q(t)\right)dt \tag{40}$$

Figure 4 shows the block diagram of the control algorithm. The control law (40) was programmed in Matlab-Simulink®, Figure 5 shows the feedback of the instantaneous position, in left is the function corresponding to the TBG, also the dynamic model is showed. The block "engine" has the control law.

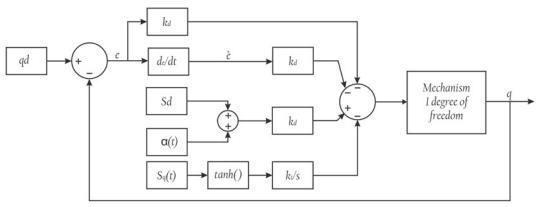

Figure 4. Diagram of the Matlab-Simulink software for joint position control with TBG

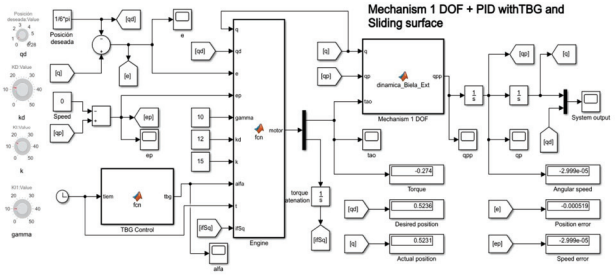

Figure 5. Diagram of the Matlab-Simulink software for joint position control with TBG

Results

This section shows the results obtained by two joint position control tests. The tests consist of bringing the mechanism from one position to a desired position in a given time.

The time base generator applies the control law to synchronize the mechanism at the desired convergence time. The TBG only adjusts the α gain in the control algorithm based on operator-specified time and does so in a transient space. The sliding surface makes the error converge more smoothly towards 0, the sliding surface has action in the transient space.

The simulations have been carried out in the Matlab-Simulink® software, using the model in Figure 5.

Test 1

The initial position of the mechanism is 0 rad and the objective is to move the mechanism to the desired position of $\pi/2$, in a finite time of 3 seconds. The α gain is adjusted based on the desired convergence time. Therefore, for this test the α gain has a constant value.

Table 2 shows the initial position, the desired position and the simulation conditions. On the other hand, Table 3 shows the tuning gains in the controller and finally the graphical results are shown below.

Table 2. Simulation data for joint control in Matlab-Simulink. Test 1

Simulation parameters	Value
Desired position (qd)	π / 2
Initial position (q)	0 rad
Solver	O de 4 (Runge-Kutta)
Convergence time (TBG)	3 s
Integration step	0.001

Table 3. Gains in the controller for joint position control in Matlab-Simulink. Test 1

Gains in the controller	Value
Gain α in TBG	10.7
Gain k	15
Gain k_d	12
Gain k_i	0.001 k_d
Gain k_p	(k_d) (α)

Figure 6 shows the evolution of the movement described by the mechanism, in the upper part the magenta line indicates the desired position, while the black line describes the change in position of the mechanism. Near second 3 a convergence between both lines is observed. Three seconds was chosen as time of arrival at the desired position and based on this the alpha gain was calculated.

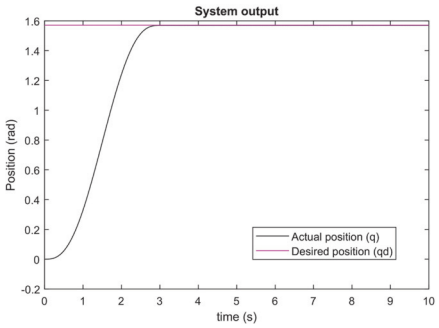

Figure 6. Plot of desired generalized variable position and initial position

Figure 6 also shows that the arrival at the desired position does not present oscillations, as shown in some conventional PID controllers. This shows that vibrations and inertial effects are eradicated with the algorithm proposed in this article.

Figure 7 shows the speed profile of the movement performed by the mechanism to reach the desired position in the proposed time. A bell-shaped speed profile has been showed, starting at time (t = 0) and gradually increasing until it reaches a maximum value at half the total movement time, at which point the speed gradually decreases until it reaches zero again.

The speed profile obtained shows that there is no over-acceleration at the beginning of the movement, thus demonstrating that the inertial effects have been canceled by the action of the control algorithm. On the other hand, the speed profile shows that the movement described by the mechanism is a smooth and precise one. During the travel time, no disturbances are observed in the speed curve, therefore, the external disturbances are also canceled by the control algorithm.

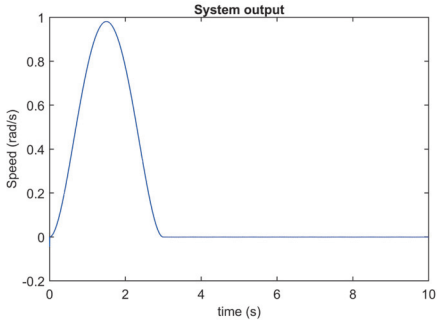

Figure 7. Plot of the bell-shaped velocity profile described by the movement of the mechanism

Figure 8 corresponds to the behavior of tau in the motor, it can be seen how tau does not present *chatter*, which again shows that the inertial effects have been canceled by the control algorithm.

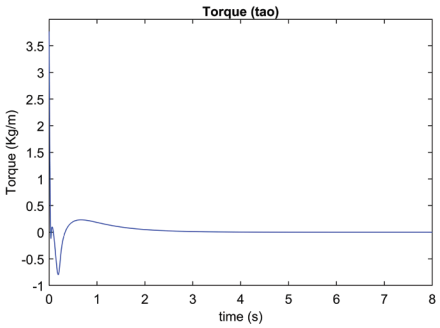

Figure 8. Engine tau plot

The Table 4 shows the results obtained in test.

Table 4. Test 1 results

Parameters	Value
Desired position	π / 2
Final position	1.56 rad.
Convergence time	3 s
Error	– 0.0015
Maximum speed	0.98 rad/s
Maximum tau	0.765 kg/m

Test 2

Test 2 is similar to test 1 with a change in some parameters to verify the functionality of the control algorithm.

Table 5 shows the initial position, the desired position and the simulation conditions, Table 6 shows the tuning gains in the controller and finally the graphical results are shown below.

https://doi.org/10.22201/fi.25940732e.2023.24.2.016

Table 5. Simulation data for joint control in Matlab-Simulink. Test 2

Simulation parameters	Value
Desired position (*qd*)	π
Initial position (*q*)	π / 2
Solver	O de 4 (Runge-Kutta)
Convergence time (*TBG*)	5 s
Integration step	0.001

Table 6. Gains in the controller for joint position control in Matlab-Simulink. Test 2

Gains in the controller	Value
Gain α in TBG	6.4
Gain k	15
Gain k_d	12
Gain k_i	0.001 k_d
Gain k_p	(k_d) (α)

As in test 1, the result of the position graph is satisfactory. The mechanism reaches the desired position in the stipulated time. There are no oscillations in the movement, indicating that the inertial effects have been canceled (Figure 9).

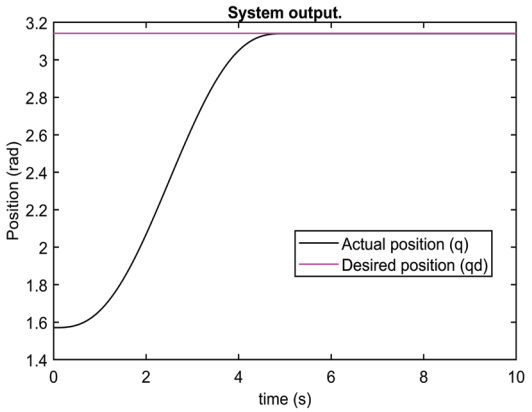

Figure 9. Plot of desired generalized variable position and initial position

The speed profile observed in Figure 10 is in agreement with what was expected. A bell-shaped velocity profile has been shown, it starts at instant zero and ends at second number 5 in accordance with the time stipulated in TBG. Let us remember that α gain is adapted according to the desired convergence time. The speed profile shows no vibrations or over acceleration.

Finally, Figure 11 shows the behavior of the tau, in the graph chattering is not observed. Table 7 shows the Test 1 results.

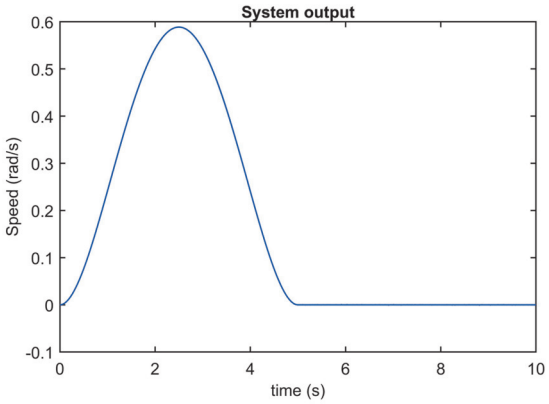

Figure 10. Plot of the bell-shaped velocity profile described by the movement of the mechanism

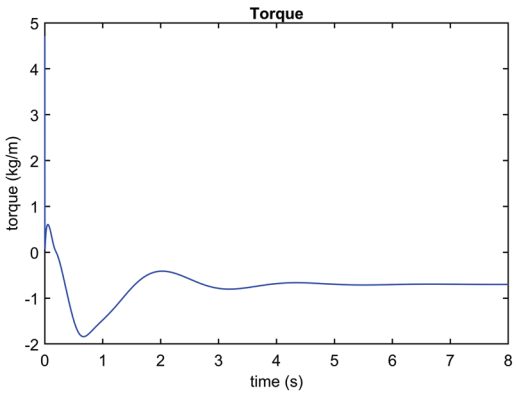

Figure 11. Engine tau plot

Table 7. Test 1 results

Parameters	Value
Desired position	π
Final position	3.142 rad
Convergence time	5 s
Error	– 0.00155
Maximum speed	0.59 rad/s
Maximum tau	0.530 kg/m

Conclusions

A robust control algorithm is introduced to cancel the inertial effects and achieve a *chatter-free* control, the algorithm has a sliding surface to ensure smooth convergence of error to zero, and a hyperbolic trigonometric function has been applied to decrease chattering. A time base generator (TBG) has been applied to reach a desired position in a finite time, in addition to obtaining a bell-shaped speed profile that ensures that over-acceleration and oscillations are eliminated when reaching the desired position. Also, a PID controller is

added to make the algorithm more robust. The algorithm can be adapted to any one degree of freedom mechanism. The bell-shaped speed profile suggests that it can be applied to robots that aim to simulate the behavior of human limbs and to future research in the field of physical rehabilitation.

References

Chen, Y., Mita, T., & Wakui, S. (1990). A new and simple algorithm for sliding mode trajectory control of the robot arm. *IEEE Transactions on Automatic Control*, 35(7), 828-829. http://doi//10.1109/9.57022.

Dominguez, O. A., Parra, V., Díaz, M. G., Pozas, M. J., & Hernandez, R. A. (2008). *Cartesian sliding PD control of robot manipulators for tracking in finite time: theory and experiments.* Vienna, Austria. http://doi//10.2507/daaam.scibook.2008.23

Feng, Y., Han, F., & Yu, X. (2014). Chattering free full-order sliding-mode control. *Automatica,* 50(4), 1310-1314. http://doi//10.1016/j.automatica.2014.01.004

Flash, T., & Hogan, N. (1985). The coordination of arm movements: An experimentally confirmed mathematical model. *The Journal of Neuroscience*, 35(7), 1688-1703. http://doi//10.1523/JNEUROSCI.05-07-01688.1985

García, L., Garelli, F., & Sala, A. (2011). Integrated sliding-mode algorithms in robot tracking applications. *Robotics and Computer-Integrated Manufacturing*, 29(1), 53-62. http://doi//10.1016/j.rcim.2012.07.007

Gashemi, M., & Nersesov, S. (2013). Sliding mode cooperative control for multirobot systems: A finite-time approach. *Mathematical Problems in Engineering*, 2013(2), 1-16. http://doi//10.1155/2013/450201

Hashimoto, H. (1993). Sliding mode control and potential fields in obstacle avoidance. European Control Conference, pp. 859-862. Groningen, Netherlands.

Huang, J., Yang, C., & Ye, J. (2014). Nonlinear PD controllers with gravity compensation for robot manipulators. *Cybernetics and Information Technologies*, 14(1), 141-150. http://doi//10.2478/cait-2014-0011

Kuo, T. C., Huang, Y. J., & Hong, B. W. (2011). Desing of adaptive sliding mode controller for robotic manipulators tracking control. *International Journal of Electrical and Computer Engineering*, 5(5), 190-194.

Morasso, P. (1981). Spatial control of arm movements. *Exp Brain Res.*, (42), 223-227. https://doi.org/10.1007/BF00236911

Morasso, P. (1993). *A dynamical model for the generation of curved trajectories. The International Conference on Artificial Neural Networks*. Amsterdam, Netherlands, 115-118.

Parra, V. A. (2003). Dynamic sliding PID control for tracking of robot manipulators: Theory and experiments. *IEEE Transactions on Robotics and Automation*, 19(6), 967-976.

Parra, V. (2001). Second order sliding mode control for robot arms with time base generators for finite-time tracking. *Dynamics and Control,* (11), 175-186. http://doi//10.1023/A:1012535929651_

Sira-Ramírez, H. (1992). On the sliding mode control of nonlinear systems. *Systems & Control Letters,* (19), 303-312. http://doi//10.1016/0167-6911(92)90069-5

Stepanenco, Y., Cao, Y., & Su, C.-Y. (1998). Variable structure control of robotic manipulator with PID sliding surfaces. *International Journal of Robust and Nonlinear Control*, (8), 79-90. http://doi//10.1002/(SICI)1099-1239(199801)8:1<79::AID-RNC313>3.0.CO;2-V

Tanaka, Y., Tsuji, T., & Kaneko, M. (1999). Biomimetic trajectory generation of robots using time base generator. International Conference on Intelligent Robots and Systems. Human and Environment Friendly Robots with High Intelligence and Emotional Quotients, 3, 1310-1315. Retrieved on http://10.1109/IROS.1999.811661.

Tanaka, Y., Tsuji, T., & Kaneko, M. (2000). A bio-mimetic rehabilitation aid for motor control training using time base generator. 2000 IEEE International Conference on Industrial Electronics, Control and Instrumentation. 21st Century Technologies, 1, 114-119. Retrieved on http://10.1109/IECON.2000.973135.

Tanaka, Y., Tsuji, T., Kaneko, M., & Morasso, P. G. (1998). Trajectory generation using time scaled artificial potential field. International Conference on Intelligent Robots and Systems. Innovations in Theory, Practice and Applications, 223-228. Victoria, Canada. Retrieved on http://doi//10.1109/IROS.1998.724623

Tsuji, T. M. (1995). Feedback control of nonholonomic mobile robots using time base generator. IEEE International Conference on Robotics and Automation. Nagoya, Japan, 1385-1390.

Tsuji, T., Morasso, P. G., & Kaneko, M. (1995). Feedback control of nonholonomic mobile robots using time base generator. IEEE International Conference on Robotics and Automation, 1995, 2, 1385-1390. Nagoya, Japan. Retrieved on http://doi//10.1109/ROBOT.1995.525471

Uno, Y., Kawato, M., & Suzuki, R. (1989). Formation and control of optimal trajectory in human multijoint arm movement. *Biological Cibernetics,* (61), 89-101. https://doi.org/10.1007/BF00204593

Yeung, S., & Chen, Y. (1988). A new controller design for manipulators using the theory of variable structure systems. *IEEE Transactions on Automatic Control*, 33(2), 200-206. http://doi//10.1109/9.391.

Zhang, D. Q., & Panda, S. K. (1999). Chattering-free and fast-response sliding mode controller. *Control Theory and Applications*, 33(2), 171-177. http://doi//10.1049/ip-cta:19990518

Cómo citar:

Suárez-Calderón J. C., Susarrey-Huerta O., Desiderio-Maya D., Rocha-Gómez I., & Flores-Campos J. A. (2023). Cancellation of inertial effects in 1 degree of freedom mechanisms applying sliding mode control with response in finite time. *Ingeniería Investigación y Tecnología,* 24 (02), 1-9. https://doi.org/10.22201/fi.25940732e.2023.24.2.016